The population of comet candidates among quasi-Hilda objects revisited and updated

J. Correa-Otto ●,★ E. García-Migani and R. Gil-Hutton★

Grupo de Ciencias Planetarias, Dpto. de Geofísica y Astronomía, FCEFyN, UNSJ - CONICET, Av. J. I. de la Roza 590 oeste, J5402DCS Rivadavia, San Juan, Argentina

ABSTRACT

In this paper, we perform a dynamical study of the population of objects in the unstable quasi-Hilda region. The aim of this work is to make an update of the population of quasi-Hilda comets (QHCs) that have recently arrived from the Centaurs region. To achieve our goal, we have applied a dynamical criteria to constrain the unstable quasi-Hilda region that allowed us to select 828 potential candidates. The orbital data of the potential candidates were taken from the ASTORB data base and we apply backward integration to search by those that have recently arrived from the outer regions of the Solar system. Then we studied the dynamical evolution of the candidates from a statistical point of view by calculating the time-averaged distribution of a number of clones of each candidate as a function of aphelion and perihelion distances. We found that 47 objects could have been recently injected into the inner Solar system from the Centaur or transneptunian regions. These objects may have preserved volatile material and are candidates to exhibit cometary activity.

Key words: celestial mechanics – comets: general – minor planets, asteroids: general.

1 INTRODUCTION

In the outer edge of the main belt there is a dynamical group called Hilda asteroids. The limits of the Hilda region are $3.7 \leq a \leq 4.2$ au in semimajor axis, $e \leq 0.3$ in eccentricity and $i \leq 20°$ in inclination. Objects in this region are near or trapped in the 3:2 mean-motion resonance (MMR) with Jupiter (Schubart 1968, 1982, 1991; Nesvorný & Ferraz-Mello 1997; Ferraz-Mello, Nesvorný & Michtchenko 1998). For the 3:2 MMR the resonant angle librates around 0 degree (Zellner, Thirunagari & Bender 1985) and for small and medium amplitudes of libration there is a stable region in the resonance known as Hilda region where reside the stable asteroids of the group. However, close to the Hilda region we can find the quasi-Hilda comets (QHCs; Kresak 1979), which could also be affected by the 3:2 MMR. The location of the QHCs is sometimes referred to as the quasi-Hilda region to indicate the dynamic difference between these objects and the Hilda asteroids. It is worth mentioning that a comet is an object characterized by its activity when it is close to the Sun.

The QHCs are Jupiter-family comets (JFCs) that have moved from outside to inside of Jupiter's orbit (Kresak 1979). Moreover, the JFCs have evolved from the transneptunian region and have reached the zone of the Jupiter orbit after suffering the perturbations of the external planets during the period they behaved as Centaurs (Fernández 1980; Duncan, Levison & Budd 1995; Levison & Duncan 1997).

However, QHCs are not the only objects inhabiting the quasi-Hilda region. There are also Hilda objects that have escaped from the stable Hilda region, which have a similar dynamic behaviour to JFCs (Di Sisto et al. 2005). As the Hilda region is located in the external zone of the main belt, where the asteroids are mainly D- and P-types, it is therefore not easy to physically distinguish them from the population of QHCs (Fitzsimmons et al. 1994; Dahlgren & Lagerkvist 1995; Dahlgren et al. 1997; Dahlgren, Lahulla & Lagerkvist 1999; Jewitt 2002; Gil-Hutton & Brunini 2008). Then, to distinguish comets from asteroids in the quasi-Hilda region, it is necessary to develop a dynamical study of the orbital evolution of these objects. The dynamical analysis of the quasi-Hilda region by Toth (2006) found new members of this cometary group, and identified 23 objects that could be dormant or extinct cometary nuclei.

Recently, coma activity has been detected in the quasi-Hilda objects 2000 YN$_{30}$ (presently known as 212P/NEAT; Cheng & Ip 2013) and (457175) 2008 GO$_{98}$ (Leonard et al. 2017), and numerical analysis indicate that in the past close encounters with Jupiter could have locked both bodies into a short-period orbit from a Centaur-like orbit. For this reason in Gil-Hutton & García-Migani (2016; GG2016 hereafter) we began a dynamical search for new QHCs candidates in the quasi-Hilda region. In that work, we identify 11 candidates (see Table 1) that had a dynamical evolution showing they could have recently arrived from the outer Solar system. One of these objects, (457175) 2008 GO$_{98}$, was analysed in García-Migani & Gil-Hutton (2018), where we confirmed cometary activity.

In this work, we follow the dynamical method described in GG2016 to update the population of QHCs that have recently arrived from the Centaur zone, which could become active near the perihelion of their orbits. In Section 2, we describe the method for the selection

Table 1. List of QHCs identified by GG2016. A small tail of dust has been detected on the asterisked object (García-Migani & Gil-Hutton 2018).

Object	Object
371837	(450807) 2007 UC$_9$
(18916) 2000 OG$_{44}$	(457175)* 2008 GO$_{98}$
(507119) 2009 SR$_{143}$	(524743) 2003 UR$_{267}$
(577805) 2013 QR$_{90}$	2001 QG$_{288}$
2002 UP$_{36}$	2006 XL$_5$
2009 KF$_{37}$	–

of the candidates and our results are presented and discussed in Section 3. Finally, our conclusions are summarized in Section 4.

2 SELECTION CRITERIA

From the ASTORB data base (Moskovitz et al. 2022) we took as pre-candidates those objects of the quasi-Hilda zone with their osculating semimajor axis in the range $3.7 \leq a \leq 4.2$ au for the epoch 2458757.5 JD (2019 October 1), and an orbit determined by more than 180 d of orbital arc length. Then, following the same criteria as the one employed in GG2016 we found a final sample of 828 asteroids in the unstable quasi-Hilda zone.

These 828 pre-candidates were numerically integrated backward over time taking into account the perturbations of all the planets of the Solar system like in GG2016. The temporal evolution of each asteroid has been solved numerically by integrating the exact equations of motion using the same N-body integrator of GG2016, which uses the Bulirsch–Stoer code with a step size of 1 d and an adopted accuracy of 10^{-13}. We found 47 new objects with a dynamical evolution that would indicate a recent income from the outer Solar system (see Table 2). This gives a total of 58 QHCs considering the 11 previously found in GG2016. An example of the possible evolution of these objects can be found in fig. 1 of GG2016, where we can see the backward evolution of (18916) 2000 OG$_{44}$. The comet first achieves Jupiter's external orbit and then it reaches the transneptunian belt after being temporally captured by several mean-motion resonances.

In the left panel of Fig. 1 are shown the 828 pre-candidates in the (a, e)-plane with the 58 QHCs candidates indicated by a red circle. We can see that almost all objects are close to the 3:2 MMR with Jupiter ($\sim$3.9607 au), whose nominal position is indicated by a vertical green line. Moreover, if we apply the simple pendulum model (see Murray & Dermott 1999) we can show the approximate position of the separatrix in blue line. We found that $\sim$98 per cent of the objects are inside the resonance. It is worth to mention that there are more sophisticated models for the study of MMRs in the literature (i.e. Gallardo 2020; Correa-Otto et al. 2021), however the pendulum model is the best option because we have only osculating elements of objects with a wide range of eccentricity and inclination values. So, the graphical representation that we present in the (a, e)-plane of Fig. 1 is not an exact dynamical picture, instead this is a simply way to show the influence of the resonance in the objects of interest.

However, the semimajor axis of the objects do not indicate the real influence of the resonance. The reason of this is that the resonant action is at its mid-point (i.e. $\sim$3.9607 au) when the resonant angle is at its maximum amplitude and when the action is at its maximum, the angle is at its centre of libration (0° for the 3:2 MMR; see Zellner, Thirunagari & Bender 1985). So, an object close to the critical semimajor axis could have a critical angle (σ) with a large

Table 2. QHCs candidates: orbital elements (2458757.5 JD) are in columns 2–4, absolute magnitude in column 5, time when the object reached $a > 5.2$ au in column 6, and last column indicate the averaged time that the clones of each candidates stay in orbits with $q < 1$ au.

Object	a au	e	i °	H	T yr	$\langle T \rangle$ yr
7458	3.730	0.172	1.76	12.0	−40913	24
30512	3.850	0.323	25.70	12.8	−18000	234
85490	3.762	0.661	2.57	14.8	−1021	589
254010	3.982	0.258	17.05	13.9	−11653	38
424570	3.980	0.223	6.62	15.5	−972	42
431336	3.776	0.244	20.40	14.9	−40212	59
508861	3.815	0.673	4.16	17.5	−8528	522
551740	4.046	0.246	24.02	15.3	−18091	149
615767	4.122	0.314	9.86	15.9	−20786	78
2000 AC$_{229}$	4.149	0.551	52.43	16.8	−30876	282
2000 CA$_{13}$	3.764	0.553	1.45	18.0	−5158	255
2002 QD$_{151}$	3.710	0.228	4.75	15.4	−925	55
2004 QR$_{38}$	3.995	0.456	11.29	16.5	−8094	207
2004 RP$_{111}$	4.174	0.622	14.14	18.2	−11713	453
2005 EC$_{272}$	3.738	0.460	7.15	16.9	−5207	133
2005 UK$_{380}$	3.899	0.370	3.03	17.8	−23579	42
2005 XR$_{132}$	3.761	0.431	14.47	16.4	−12682	51
2007 RM$_{150}$	3.856	0.446	11.11	16.1	−18286	167
2008 QZ$_{44}$	4.195	0.441	11.35	17.1	−727	237
2008 SZ$_{283}$	3.961	0.417	14.80	17.2	−100	260
2009 QM$_{24}$	3.784	0.427	13.75	16.4	−1007	130
2009 TC$_{54}$	3.817	0.373	5.87	16.4	−1765	131
2010 ES$_{189}$	4.103	0.364	31.61	15.6	−2425	445
2010 JB$_{184}$	3.977	0.284	21.18	16.4	−2897	136
2011 DL$_{12}$	3.829	0.329	13.48	16.7	−1163	137
2011 MX$_9$	4.103	0.475	19.23	16.7	−15789	445
2011 QQ$_{99}$	3.801	0.426	3.21	16.5	−420	79
2011 UB$_{301}$	3.801	0.334	21.13	17.0	−10827	61
2011 UG$_{104}$	3.993	0.407	29.59	16.2	−4030	175
2011 US$_{383}$	3.827	0.365	7.87	16.8	−4088	22
2011 WD$_{180}$	3.884	0.399	15.69	18.0	−7447	146
2014 MZ$_{101}$	4.110	0.365	17.62	16.3	−1478	152
2014 OM$_{449}$	3.993	0.284	19.81	18.0	−31963	54
2014 VF$_{40}$	3.757	0.492	24.48	16.3	−4430	332
2015 PV$_{306}$	4.109	0.294	12.41	15.3	−900	103
2016 CD$_9$	3.707	0.407	5.92	17.3	−3060	52
2016 JF$_{46}$	3.778	0.260	16.17	16.1	−331	257
2016 NQ$_{77}$	3.829	0.429	13.09	17.2	−5797	74
2016 WP$_{51}$	3.950	0.434	14.98	16.9	−3348	92
2016 BS$_{30}$	3.827	0.346	11.66	15.8	−5646	36
2017 FU$_{158}$	3.725	0.679	23.84	19.1	−2373	560
2018 PE$_{48}$	3.738	0.332	12.74	17.0	−10630	17
2019 JB$_{49}$	3.852	0.265	10.52	16.5	−757	63
2020 FV$_{35}$	3.813	0.305	4.12	17.0	−1041	137
2020 UO$_{43}$	4.139	0.645	1.75	18.7	−565	563
2020 XH$_{11}$	4.032	0.276	27.53	16.6	−6247	599
2021 JF$_{52}$	3.932	0.565	24.75	16.2	−34527	359

amplitude, and therefore, it is not really close to the centre of the MMR.

Hence, we can represent the distribution of the candidates in the (a, σ)-plane by calculating the osculating value of the characteristic or resonant angle σ. Fig. 1 shows in the right panel the distribution of the 828 pre-candidates, with the QHCs candidates indicated by a red circle. We found here an interesting result: while the other quasi-Hildas objects can be placed anywhere in the plane, the 58 QHCs candidates are placed far from the resonant centre. We can define a limit in semimajor axis of $\sim$±0.06 au from the central or
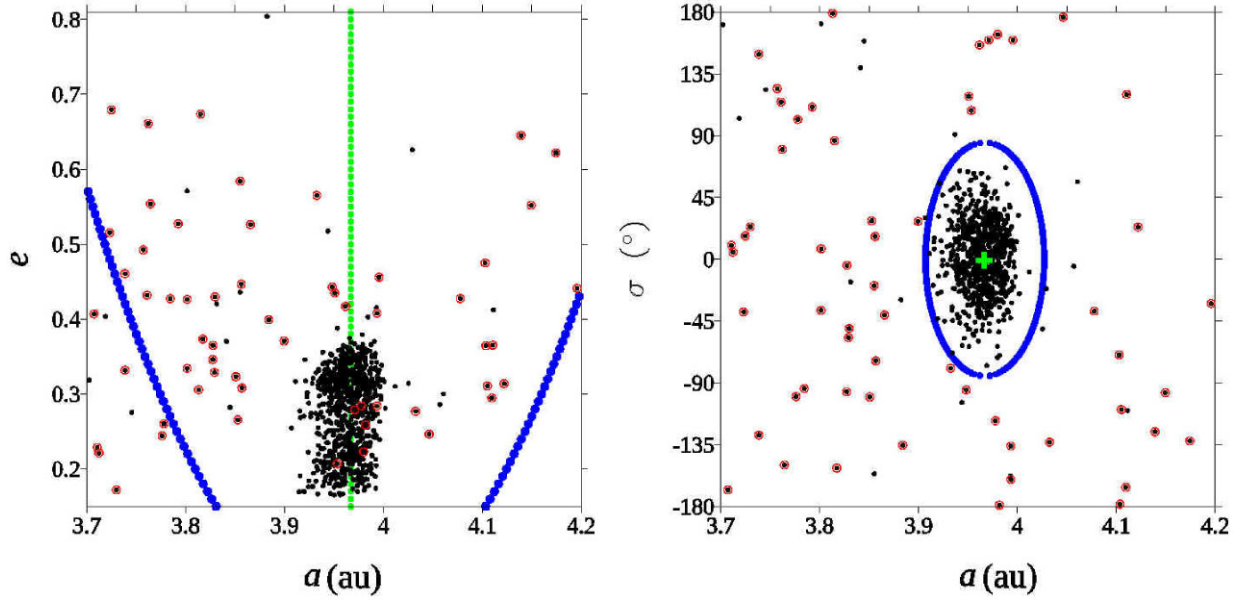
Figure 1. Left panel: Distribution of the pre-candidates in the (a, e)-plane, the nominal position of the resonance is indicated by a vertical line and the limits of the resonance are also indicated. Right panel: Distribution of the pre-candidates in the (a, σ)-plane, the centre of the resonance is indicated by a cross. The QHCs candidates are indicated by a circle. We can see that the QHCs candidates are in the periphery of the MMR, beyond the ellipse in right panel.

nominal value ($a_0 \sim 3.9607$ au) and a limit of $\sim \pm 90°$ in the resonant angle, and we can see that there are no QHCs candidates within the mentioned limits. This important result allows us to predict where we could find new QHCs candidates. Following Toth (2006), we can define a region inside the unstable quasi-Hilda zone where the cometary objects can be found, and from the distribution of real objects we can propose the following empirical criteria for the limits in the (a, σ)-plane:

$$\sigma = \pm 90 \sqrt{1 - \left(\frac{a - a_0}{0.06}\right)^2}, \tag{1}$$

this ellipse is plotted in blue in the right panel of Fig. 1. Then, the objects outside the ellipse are the possible QHCs candidates, and the objects inside the ellipse can be discarded.

3 RESULTS

The recent dynamical history of the 58 objects of Tables 1 and 2 would indicate that they were Centaurs or transneptunian objects that evolve towards their actual position in the 3:2 MMR and ended as QHCs. However, the evolution of these objects is chaotic because they cross several MMRs and some of them have close approaches with Jupiter and other planets. Therefore, these chaotic orbits are sensitively dependent on initial conditions and the integration method employed (i.e. Bulirsch–Stoer or Radau). As in GG2016, the dynamical study of chaotic orbits could be developed from a statistical point of view by following the backward temporal evolution of clones of each object. These clones can be generated by small changes in the initial osculating orbital elements of each object like the initial conditions generated to calculate the maximum Lyapunov characteristic exponent (Murray & Dermott 1999).

As in GG2016, we study the dynamical evolution of the 47 new QHCs candidates by mapping the time-averaged distribution of 100 clones of each candidate in the plane of aphelion and perihelion distances, or the (Q, q)-plane (e.g. Tiscareno & Malhotra 2003). It is

difficult to present the (Q, q)-planes corresponding to each candidate and, since we observe similar dynamical characteristics in all planes, we present the results of some QHCs candidates as examples. Then, in Fig. 2 we show the results of 9 QHCs candidates as examples of the main dynamical characteristics observed after a backward integration of 50 kyr.

The results observed in the density maps of each one of the 47 QHCs candidates are similar and present the same characteristics obtained by GG2016 for their 11 candidates. We found a dynamical behaviour consistent with objects coming from the outer Solar system (i.e. Centaur or transneptunian regions) that reach the quasi-Hilda region through the gravitational scattering of the giant planets. For the 9 candidates taken as examples in Fig. 2, we can see how Jupiter and Saturn produce a gravitational scattering over the clones, increasing their aphelion distances. These can be appreciated in the horizontal strips of density with almost constant perihelion distances at $q \sim 5.2$ au and 9.5 au, which we have indicated by dotted horizontal lines. We can see an important density accumulation in the horizontal strip corresponding to Jupiter, and a lower density build-up in the strip corresponding to Saturn. This is due to the short time of integration of our simulations (50 kyr), the particles start closer to Jupiter and take more time to reach Saturn. Moreover, the time-scales of particle ejection for Jupiter are shorter than that for Saturn. Numerical simulations with longer integration times would allow the particles to reach Neptune's orbit in a dynamical behaviour similar to that founded in Tiscareno & Malhotra (2003) for the Centaurus population.

Moreover, almost all the 47 candidates studied are able to visit the region below 1 au where the comets could show intense activity. In Fig. 2, we indicate the limit $q = 1$ au with a horizontal dotted line. As in GG2016 we calculate the averaged time that the clones of the QHCs candidates stay in orbits with a perihelion distance lower than 1 au ($<T>$), showing the result for each object in the last column of Table 2. As it is explained in GG2016, there is a high probability that a comet will become inactive if it remains in an orbit with $q < 1$ au for at least 1 kyr. Then, QHCs candidates with a large average
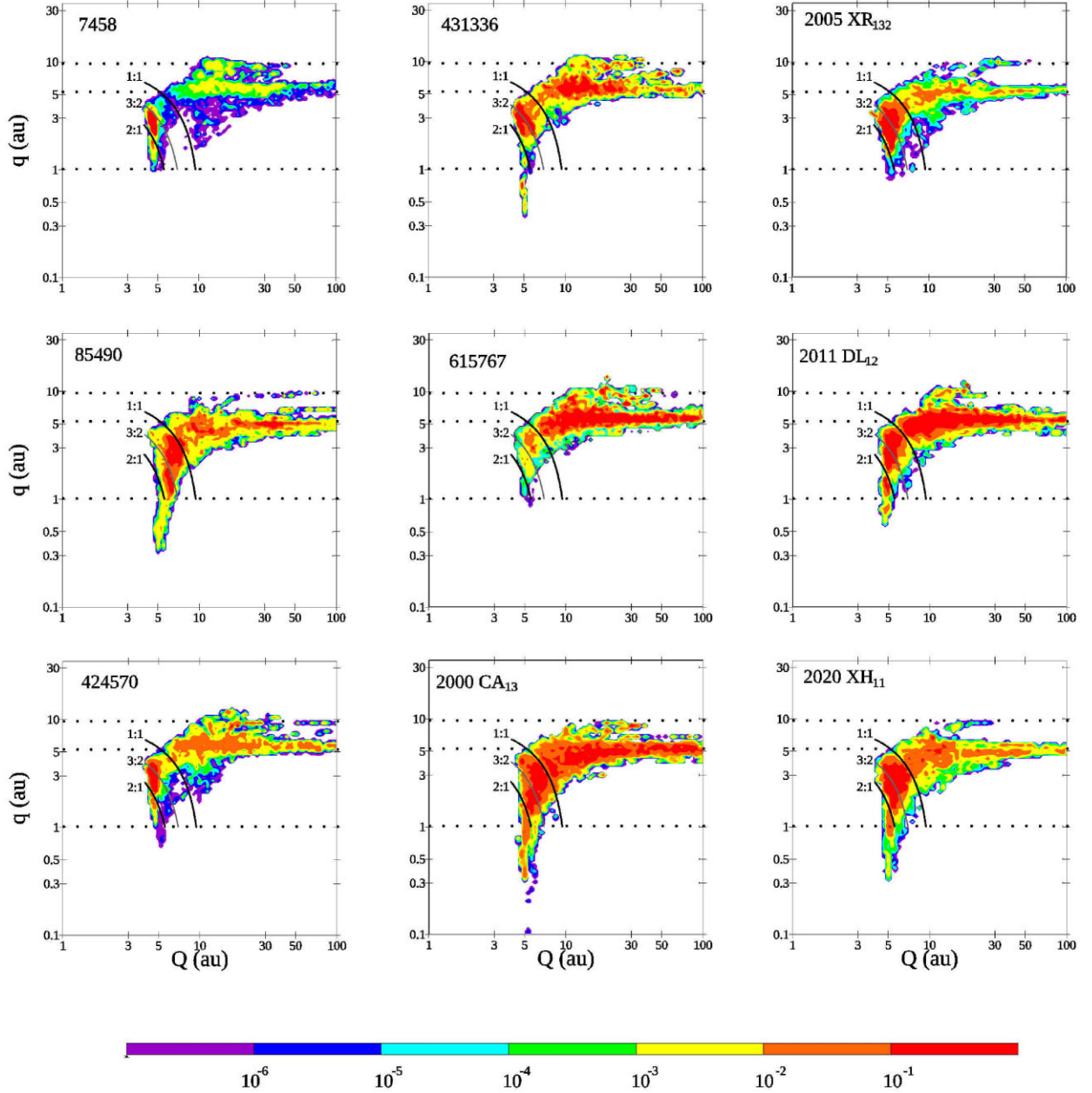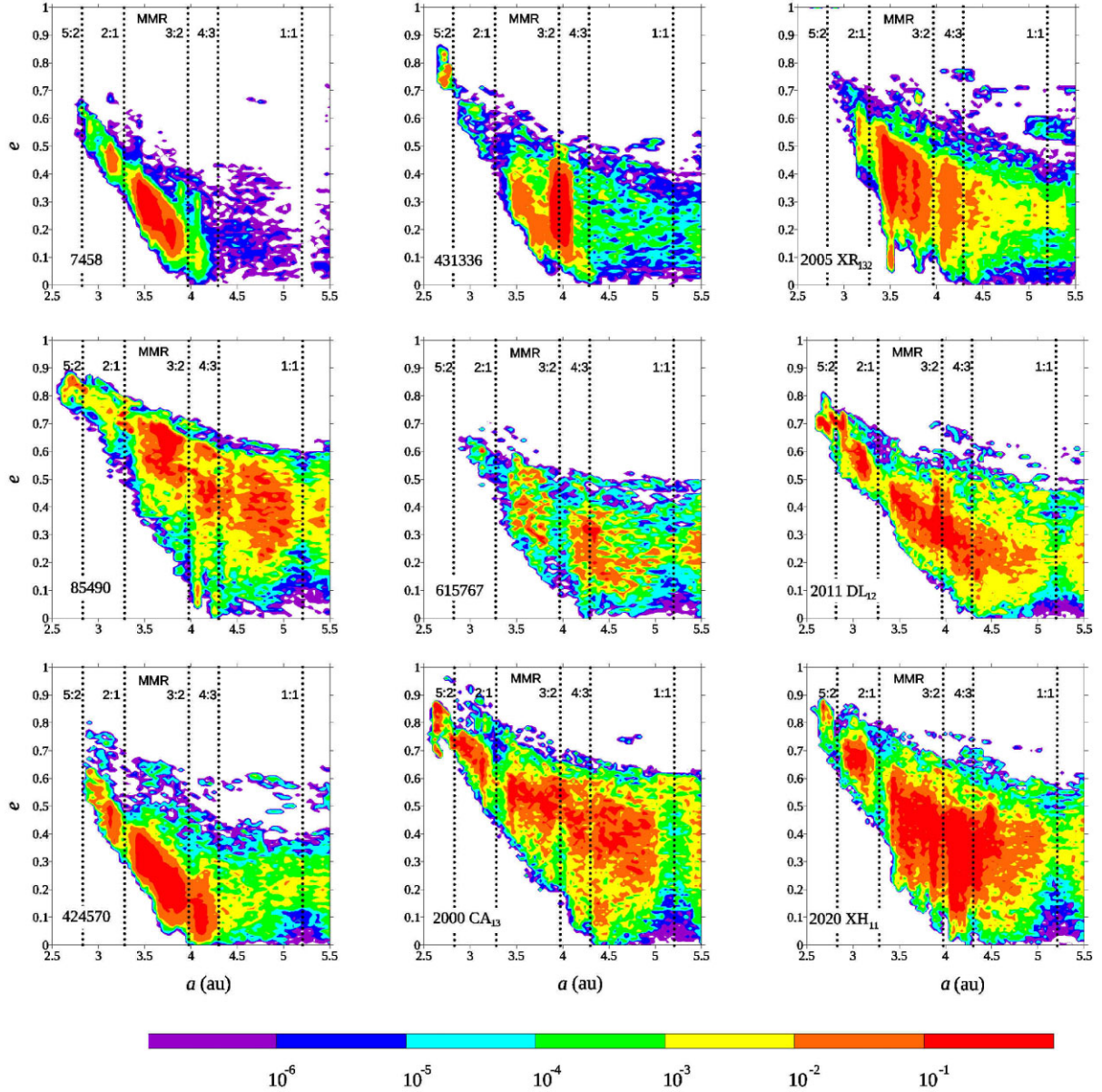
Figure 2. Probability distribution in the (Q, q)-plane for the clones of 9 candidates: 7458, 85490, 424570, 431336, 615767, 2000 CA$_{13}$, 2005 XR$_{132}$, 2011 DL$_{12}$, and 2020 XH$_{11}$. Dotted lines indicate perihelion distance of 9.5, 5.2, and 1 au. Continuous lines indicate the 1:1 MMR, the 2:1 MMR, and the 3:2 MMR.

time in orbits with $q < 1$ au have a high probability of being dormant or extinct cometary nuclei. Thus, that objects with $<T>$ less than ~ 200 yr are the most probable QHCs candidates that have recently arrived at the quasi-Hilda region and the best objects to search signals of activity due to outgassing. There are 28 candidates meeting this condition, which represent ~ 60 per cent of the sample of 47 QHCs candidates, a similar fraction to that obtained by GG2016 for their sample. Therefore, these objects represent an important opportunity to find more QHCs and to confirm the QHCs candidates.

On the other hand, as the clones start in a position close to the 3:2 MMR and then evolve through a process of slow diffusion we can see a bulk of density around this resonance. In Fig. 2, we indicate the nominal position of the 3:2 MMR by a grey line and we also include the nominal position of the 2:1 MMR ($a \sim$

3.27 au) and the 1:1 MMR with black lines as reference. Then, to see in more details the dynamical characteristics of the evolution of these particles in the region $a < 5.2$ au, we represent the time-averaged distribution of the 100 clones of each candidate in the (a, e)-plane with limits $a \in (2.5, 5.5)$ au, and $e \in (0, 1)$. These results are present in Fig. 3, where we also include the nominal position of the 5:2 (~ 2.82 au), 2:1 (~ 3.27 au), 3:2 (~ 3.96 au), 4:3 (~ 4.3 au), and 1:1 MMRs with Jupiter as vertical dotted lines. As the clones start in a position close to the 3:2 MMR, we start with the analysis of this resonance. For some maps, we can see a region of low density in the nominal position of the 3:2 MMR (i.e. 7458, 85490, 2005 XR$_{132}$), while other maps show a zone of high density (i.e. 431336, 2011 DL$_{12}$). This suggests that in some cases the 3:2 MMR is capable of transiently trapping clones. Instead, in all the

Figure 3. Probability distribution in the (a, e)-plane for the clones of 9 candidates: 7458, 85490, 424570, 431336, 615767, 2000 CA$_{13}$, 2005 XR$_{132}$, 2011 DL$_{12}$, and 2020 XH$_{11}$. Vertical dotted lines indicate the nominal position of the main MMRs with Jupiter.

cases we can see a region of low density around the 1:1 MMR and around the 2:1 MMR. These results suggest that the clones cross these resonances without ever being trapped, in contrast to the 3:2 MMR. Moreover, the dynamic evolution of the clones does not seem to be significantly affected by the 4:3 MMR. For this resonance, we neither see an accumulation that would indicate a temporary trapping nor a significant gap in the density. Finally, the clones reach the region of 3 au with a high eccentricity of ∼0.6 (i.e. $q \sim 1.2$ au). Therefore, only the clones able to cross the 5:2 MMR (∼2.82 au) could achieve the inner zone of the Solar system. However, it is worth noting that this resonance should not be understood as a barrier but as a reference to identify the candidates that can reach distances less than 1 au.

4 CONCLUSIONS

In this article, we continue with the identification of QHCs candidates, initiated in GG2016. From the ASTORB data base we have selected 828 pre-candidates to QHCs in the quasi-Hilda region, which were dynamically analysed in order to find those that could have arrived from the Centaur region. The criteria used to select our sample were the same as those used in GG2016: i) $a \in (3.7, 4.2)$ au, ii) orbital arcs spanned by the observations greater than 180 d, and iii) the criteria of Toth (2006) for unstable orbits apply to Lagrangian elements. Each pre-candidate was numerically integrated for a backward time-span of 50 kyr, considering the perturbation of all the planets in the Solar system and with the object assumed to be a massless body.

We report 47 QHCs candidates after our dynamical study. The backward integration of the orbit of each object showed a dynamical evolution from the quasi-Hilda region toward the Centaur zone. This recent arrival of our candidates has taken place in a rather chaotic way due to the perturbation of the giant planets, so we have complemented the dynamical study of our candidates with a statistical analysis of the evolution of their orbits. Moreover, with our 47 candidates and the 11 reported by GG2016, we were able to define an empirical criterion in the resonance plane, which allows us to define a region where the QHCs candidates are most likely to be found.

From the results obtained, we can deduce that all the QHCs candidates are able to visit the inner region of the Solar system and those with $<T>$ larger than 200 yr ($\sim$40 per cent of the candidates) could be affected by strong activity and occasionally become inactive comets. Instead, the candidates whose clones remain below 1 au for a short time are more likely to still be active. Therefore, during the following 2–3 yr, it is interesting to follow their orbits when they will pass by the perihelion because during that period they offer a good opportunity to detect activity.

ACKNOWLEDGEMENTS

DATA AVAILABILITY

Table 2 indicates all the QHCs candidates and their main dynamical characteristics founded in our research. Moreover, the main results of the clones of some QHCs candidate are available in Figs 2 and 3. The obtained results for the other candidates and their clones will be shared on request to the corresponding author.

REFERENCES

Cheng Y. C., Ip W. H., 2013, AJ, 770, 97
Correa-Otto J. A., Cañada-Assandri M., García R. S., Trógolo N. E., Leiva A. M., Gil-Hutton R., 2021, Icarus, 367, 114564
Dahlgren M., Lagerkvist C. I., 1995, A&A, 302, 907
Dahlgren M., Lagerkvist C. I., Fitzsimmons A., Williams I. P., Gordon M., 1997, A&A, 323, 606
Dahlgren M., Lahulla J. F., Lagerkvist C. I., 1999, Icarus, 138, 259
Di Sisto R. P., Brunini A., Dirani L. D., Orellana R. B., 2005, Icarus, 174, 81
Duncan M. J., Levison H. F., Budd S. M., 1995, AJ, 110, 3073
Fernández J. A., 1980, MNRAS, 192, 481
Ferraz-Mello S., Nesvorný D., Michtchenko T. A., 1998, in Lazzaro D., Vieira Martins R., Ferraz-Mello S., Fernandez J., Beauge C., eds, ASP Conf. Ser. Vol. 149 Solar System Formation and Evolution. Astron. Soc. Pac., San Francisco, p. 65
Fitzsimmons A., Dahlgren M., Lagerkvist C. I., Magnusson P., Williams I. P., 1994, A&A, 282, 634
Gallardo t., 2020, Celest. Mech. Dyn. Astron., 132, 9
García-Migani E., Gil-Hutton R., 2018, Planet. Space Sci., 160, 12
Gil-Hutton R., Brunini A., 2008, Icarus, 193, 567
Gil-Hutton R., García-Migani E., 2016, A&A, 590, A111 (GG2016)
Jewitt D. C., 2002, AJ, 123, 1039
Kresak L., 1979, in Gehrels T., ed., Asteroids. Univ. Arizona Press, Tucson, p. 289
Leonard G. J. et al., 2017, Minor Planet Circ., N50
Levison H. F., Duncan M. J., 1997, Icarus, 127, 13
Moskovitz N. A.,Wasserman L.,Burt B.,Schottland R.,Bowell E., Bailen M., Granvik M., 2022, The astorb database at Lowell Observatory, Astronomy and Computing, 41, 65
Murray C. D., Dermott S. F., 1999, Solar System Dynamics. Cambridge Univ. Press, Cambridge
Nesvorný D., Ferraz-Mello S., 1997, Icarus, 130, 247
Schubart J., 1968, AJ, 73, 99
Schubart J., 1982, A&A, 114, 200
Schubart J., 1991, A&A, 241, 297
Tiscareno M. S., Malhotra R., 2003, AJ, 126, 3122
Toth I., 2006, A&A, 448, 1191
Zellner B., Thirunagari A., Bender D., 1985, Icarus, 62, 505

This paper has been typeset from a TEX/LATEX file prepared by the author.